Synthesis, characterization, solvatochromic, antioxidant and antibacterial activities investigation of 2,2'-((1E,1'E)-((1,2,5-oxadiazole-3,4-diyl)bis (azanylylidene))bis(methanylylidene))bis(4-(phenyldiazenyl)phenol)

ABSTRACT

The azo-azomethine dyes 2-[(4-amino-1,2,5-oxadiazol-3-ylimino)methyl)-4-(phenyl diazenyl]phenol (**2a-h**) have been synthesized from the condensation reaction of 3,4-diamino -1,2,5-oxadiazole with 2-hydroxy-5-[(E)-(aryldiazenyl)]benzaldehyde(**1a-h**) in methanol. The structures of dyes have been characterized by elemental analysis, mass, IR, UV-Vis, ^{1}H and ^{13}C NMR spectroscopy. UV–Vis absorption spectra indicated enol–keto tautomeric and positive solvatochromism in compounds **2a-h** which is dependent on the substitution, solvent, pH and environment temperature. The synthesized compounds were investigated for their *in vitro* antioxidant activity by 1,1-diphenyl-2-picrylhydrazyl (DPPH) assay. Compounds substituted with electron donating groups, such as, alkyl and methoxy groups showed moderate to mild antioxidant activity. The *in-vitro* antibacterial activity of all compounds was determined by disc diffusion method. The tested compounds showed varying degree of inhibition against *B. cereus* and *S. aureus* strains. However, *E.coli* and *K. pneumonia* were not sensitive to any of the tested samples.

Keywords: Azo-azomethine, Azo-dyes, Schiff base, Solvatochromism, antioxidant activity, antibacterial activity.

1. Introduction

The azo-azomethine dyes are considered privileged compounds because they are easily prepared by the condensation between amines and aldehyde or ketones [1]. A large number of azo-azomethines have been synthesized for their interesting properties e.g. light emittion diode (LED)[2-5], corrosion inhibitor [6], potentiometric sensor [7], intermediate to obtained of some heterocyclic compounds [8], to synthesize of conjugate polymers containing azomethine [9], and their wide spectrum biological actives and used in drugs and cosmetics [10, 11]. Also, these compounds have been used as dyestuffs for wool, leather and synthetic materials because of their extraordinary coloring properties and in photonic devices [2-5, 11]. Some of metal complexes of azo-azomethine have been widely used in technology due to their photo physical and energy-transfer properties [5, 7, 12]. Furthermore, the oxadiazoles are important compounds that have many derivatives with wide range of interesting properties, such as synthesis of condensed compounds heterocyclic systems, antibacterial, antifungal, analgesic, anti-inflammatory, antiviral, anticancer, antihypertensive, anticonvulsant, and anti-diabetic properties [13-16]. Also, the 2-hydroxy Schiff bases have enol and keto form in their proton tautomeric structure and enol form is usually more stable [8, 12, 17, 18]. The keto form stabilized by hydrogen bonding and electrostatic intermolecular interactions [17-20]. We reported recently synthesis, solvatochromism, antibacterial activity of 2-[(4-amino-1,2,5-oxadiazol-3-ylimino)methyl)-4-(phenyldiazenyl]phenol [20]. In this article, our interest is focused on preparation of symmetrical azo-azomethine dyes of 2,2'-(1E,1'E)-(1,2,5-oxadiazole-3,4-diyl)bis(azan-1-yl-1-ylidene)bis(methan-1-yl-1-ylidene)bis(4-(phenyldiazenyl)phenol (**2a-h**) with three objectives: (i) Synthesis of oxadiazole-based azo-azomethine dyes, (ii) Study of biological properties of synthesized compounds, (iii) Study of solvatochromic behavior and substituent effects of the prepared dyes in various solvents.

Experimental

2.1. Materials and Measurements

All chemical reagents were obtained from the Merck and used without further purification. 2-hydroxy-5-(aryldiazenyl))benzaldehyde (**1a-h**) and 3,4-diamino-1,2,5-oxadiazole have been prepared and purified according to the method reported in the literature [8, 12, 17-20]. Melting points were measured with Electrothermal 9300 apparatus. Elemental analyses were performed on an Elementar Vario EL III elemental analyzer. Mass spectra were recorded on a Agilent MS Model 5973. The IR spectra were recorded with a Shimadzu 8400 S spectrometer. The structure of synthesized compounds was confirmed by ^{1}H and ^{13}C NMR spectra, in DMSO-d_6 as solvent on a Bruker AV 300 MHz spectrometer. The pH variation experiments were carried out in a microprocessor pH meter (HANNA 211 pH) at constant temperature (298 K). The UV-vis. spectra were recorded with a Shimadzu 1650 spectrophotometer. In order to obtain UV–vis. spectra, 2.5 mL of a 0.001 M solution of the synthesized ligand was transferred into a 1.00 cm quartz cell and titrated with a concentrated solution of potassium hydroxide using a 100-µL Hamilton syringe. Each spectrum was recorded immediately after the titrant addition.

*2.2. General procedure for Synthesis of 2,2'-(1E,1'E)-(1,2,5-oxadiazole-3,4-diyl)bis(azan-1-yl-1-ylidene)bis(methan-1-yl-1-ylidene)bis(4-(phenyldiazenyl)phenol (**2a-h**)*

To a stirring solution of 2-hydroxy-5-(aryldiazenyl))benzaldehyde (**1a-h**, 20 mmol) in methanol (300 mL), a solution of 3,4-diamino-1,2,5-oxadiazole (1.20 g, 12 mmol) in methanol (10 mL) was added at 60-70 ºC. The solution was stirred for 1 h at 60-70 ºC and was added acetic acid (0.10 g of 98% aqueous solution, 2 mmol). The mixture was stirred and refluxed for 8 h at 60-70 ºC. The solution was then concentrated to a volume of ca. 20 mL and precipitate filtered.

Compound **2a**: The brown product is soluble in CH_3OH, C_2H_5OH, DMSO, DMF and crystallized from a 1:1 mixture of THF. Yield, 3.65 g(70.74 %). m.p.281-282 ºC. FT-IR (KBr, cm^{-1}): 3429 *ν*(OH), 1610 *ν*(C=N), 1573 *ν*(N=N),1483 *ν*(C=C), 1284 *ν*(C-N), 1191 *ν*(C-N), 1110 *ν*(Ar-O), 1037 *ν*(N-O). ^{1}H NMR, ppm: 11.82(2H, OH, D_2O exchangble), 9.46(s, 2H, C<u>H</u>=N), 8.51(bs, 2H), 8.06, 8.03(d, 2H, J=8.50 Hz), 7.82, 7.80(d, 4H, J=6.72 Hz), 7.52, 7.50(d, 6H, J=5.79), 7.20, 7.17(d, 2H, J=8.83 Hz). ^{13}C NMR, ppm: 167.02, 162.81, 156.48, 151.86, 145.02, 131.10, 128.91, 124.40, 124.36, 122.39, 120.81, 118.05. The EI-MS: m/z 516$(M)^+$, 515$(M-1)^+$, 514$(M-2)^+$, 292, 224, 105. Anal. Calcd. for $C_{28}H_{20}N_8O_3$: C, 65.11; H, 3.90; N, 21.69. Found: C, 65.02; H, 3.82; N, 21.50.

Compound **2b**: The brown product is soluble in DMSO, DMF and crystallized from THF. Yield, 3.42 g(62.87 %). m.p.270-271 ºC. FT-IR (KBr, cm^{-1}): 3435 *ν*(OH), 2930, 2856 *ν*(C<u>H</u>=N), 1612 *ν*(C=N), 1577 *ν*(N=N),1483 *ν*(C=C), 1340, 1284 *ν*(C-N), 1191 *ν*(C-N), 1103 *ν*(Ar-O), 1014, 923 *ν*(N-O). ^{1}H NMR, ppm: 11.90(2H, OH, D_2O exchangble), 9.46(s, 2H, C<u>H</u>=N), 8.49, 8.48 (d, 2H, J=2.43 Hz), 8.05, 8.04, 8.02, 8.01(dd, 2H, J= 2.48 Hz), 7.74, 7.72(d, 4H, J=8.2 Hz), 7.32, 7.29(d, 4H, J=8.11 Hz), 7.25, 7.23(d, 2H, J=8.90 Hz), 2.35(s, 6H). ^{13}C NMR, ppm: 166.95, 162.58, 156.55, 149.95, 144.97, 141.21, 131.34, 129.90, 123.88, 122.40, 120.80, 118.07, 21.00(CH_3). The EI-MS: m/z 545$(M+1)^+$, 544$(M)^+$, 543$(M-1)^+$, 540, 528, 426, 307, 265, 239, 212, 120, 107, 92. Anal. Calcd. for $C_{30}H_{24}N_8O_3$: C, 66.17; H, 4.44; N, 20.58. Found: C, 66.08; H, 4.36; N, 20.42.

Compound **2c**: The orange product is soluble in DMSO, DMF and crystallized from CH_3CN. Yield, 3.86 g(62.87 %). m.p.273-274 ºC. FT-IR (KBr, cm^{-1}): 3465 *ν*(OH), 2958, 2869 *ν*(C<u>H</u>=N), 1604 *ν*(C=N), 1521 *ν*(N=N), 1479 *ν*(C=C), 1338, 1280 *ν*(C-N), 1193 *ν*(C-N), 1153 *ν*(Ar-O), 1045, 931 *ν*(N-O). ^{1}H NMR, ppm: 11.87(2H, OH, D_2O exchangble), 9.46(s, 2H, C<u>H</u>=N), 8.48(bs, H), 8.04, 8.01(d, H, J=7.41 Hz), 7.81, 7.78(d, 2H, J=7.18 Hz), 7.76, 7.73(d,

4h, J=7.93 Hz), 7.43, 7.40(d, 2H, J=7.18 Hz), 7.37, 7.34(d, 4H, J=8.09 Hz), 7.21, 7.18(d, 2H, J=8.75 Hz), 294-2.90(q, 4H, J=6.75 Hz), 1.23-1.18(t, 6H, J=6.75 Hz). ^{13}C NMR, ppm: 167.05, 163.80, 156.45, 150.25, 144.85, 128.87, 124.05, 122.47, 120.77, 118.15, 23.65(CH_2), 13.37(CH_3).

Compound **2d**: The orange product is soluble in CH_3OH, C_2H_5OH, THF, DMSO, DMF and crystallized from a 1:1 mixture of THF/CH_3CN. Yield, 4.34 g(75.87%). m.p.199-200 ºC. FT-IR (KBr, cm^{-1}): 3452 *v*(bs, OH), 2918, 2848*v*(Ar-H), 1622 *v*(C=N), 1622, 1581 *v*(N=N), 1488 *v*(C=C), 1282 *v*(C-N), 1101 *v*(Ar-O), 1039, 941 *v*(N-O). ^{1}H NMR, ppm: 11.81(2H, OH, D_2O exchangble), 9.40 (s, 2H, C<u>H</u>=N), 8.46 (s, 2H), 8.02, 7.99(d, 2H, J=8.85 Hz), 7.39(s, 4H), 7.17, 7.14(d, 2H, J=8.85 Hz), 7.09(s, 2H), 2.28 (s, 12H). ^{13}C NMR, ppm: 167.10, 162.75, 156.38, 152.04, 145.17, 138.63, 132.54, 129.02, 124.32, 120.80, 120.30, 118.03, 20.88(CH_3). Anal. Calcd. for $C_{32}H_{28}N_8O_3$: C, 67.12; H, 4.93; N, 19.57. Found: C, 66.96; H, 4.88; N, 19.52. The EI-MS: m/z 574$(M+2)^+$, 572$(M)^+$, 570$(M-2)^+$, 555, 440, 348, 322, 252, 225, 133, 106, 78.

Compound **2e**: The brown product is soluble in CH_3OH, C_2H_5OH, THF, DMSO, DMF and crystallized from CH_3OH. Yield, 4.34 g(75.87%). m.p.275-276 ºC. FT- IR (KBr, cm^{-1}): 3460 *v*(bs, OH), 2964, 2871*v*(Ar-H), 1600 *v*(C=N), 1525 *v*(N=N), 1481 *v*(C=C), 1284 *v*(C-N), 1110 *v*(Ar-O), 1037, 962 *v*(N-O).

Compound **2f**: The brown product is soluble in CH_3OH, C_2H_5OH, THF, DMSO, DMF and crystallized from CH_3OH. Yield, 4.34 g(75.87%). m.p.274-277 ºC. FT- IR (KBr, cm^{-1}): 3461 *v*(bs, OH), 2939, 2840*v*(Ar-H), 1654 *v*(C=N), 1583 *v*(N=N), 1473 *v*(C=C), 1278 *v*(C-N), 1107 *v*(Ar-O), 1033, 907 *v*(N-O).

Compound **2g**: The red product is soluble in DMSO, DMF and crystallized from THF. Yield, 3.22 g(53.14%). m.p.295-296 ºC. FT-IR (KBr, cm^{-1}): 3431 *v*(bs, OH), 2926, 2881 *v*(Ar-H), 1633 *v*(C=N), 1578 *v*(N=N), 1478 *v*(C=C), 1521 *v*(N=O, Unsym. Stretching), 1335 *v*(N=O, Sym. Stretching), 1286 *v*(C-N), 1147 *v*(Ar-O), 1103, 912 *v*(N-O). ^{1}H NMR, ppm: 11.89(2H, OH, D_2O exchangble), 10.58(s, 2H, C<u>H</u>=N), 8.71(m, 2H), 8.36, 8.33(d, 4H, J=7.94 Hz), 8.18-8.07(m, 2H), 7.92, 7.88(d, 4H, J=7.94 Hz), 7.22(m, 2H). ^{13}C NMR, ppm: 169.42, 163.80, 156.72, 152.12, 149.96, 143.68, 129.78, 126.79, 124.08, 122.44, 122.04, 117.98. Anal. Calcd. for $C_{28}H_{18}N_{10}O_7$: C, 55.45; H, 2.99; N, 23.09. Found: C, 55.36; H, 2.86; N, 23.00. The EI-MS: m/z 608$(M+2)^+$, 607$(M+1)^+$, 606$(M)^+$, 561, 457, 365, 353, 338, 308, 243, 138, 123.

Compound **2h**: The Orang product is soluble in CH_3OH, C_2H_5OH, THF, DMSO, DMF and crystallized from diethyl ether or THF. Yield, 4.00 g(59.00 %). m.p.>300 ºC(dec). FT-IR (KBr, cm^{-1}): 3442 *v*(OH), 3072 *v*(Ar-H), 1652 *v*(C=N), 1574 *v*(N=N),1481 *v*(C=C), 1284 *v*(C-N), 1222 *v*(S=O, Unsym. Stretching), 1184 *v*(S=O, Sym. Stretching), 1155 *v*(Ar-O), 1037 *v*(N-O), 680 *v*(S-O-H, Unsym, Stret.), 630 *v*(S-O-H, Sym. Stret.). ^{1}H NMR, ppm: 11.57, 1156(4H, OH, D_2O exchangble), 10.35(s, 2H, C<u>H</u>=N), 8.19-7.17(m, 14H, Ar-H). ^{13}C NMR, ppm: 171.83, 163.50, 157.48, 151.53, 150.43, 144.76, 129.80, 126.72, 123.85, 122.64, 121.94, 118.49. The EI-MS: m/z 676$(M)^+$, 628, 604, 576, 551, 536, 515, 490, 368, 313, 299, 265, 185, 97 . Anal. Calcd. for $C_{28}H_{20}N_8O_9S_2$: C, 49.70; H, 2.98; N, 16.56; S, 9.48. Found: C, 49.56; H, 2.84; N, 16.46; S, 9.32.

2.4.1. Antioxidant Activity

The *in vitro* Antioxidant activity of **2(a-h)** was investigated by DPPH assay [21]. 200 µL of test compounds in DMSO (1mg/mL) was mixed with 4mL of 6×10^{-5}M DPPH in methanol. These solutions were vortexed vigorously and kept in dark at RT for 30 min. The control contained all reagents without the compound. DPPH radical scavenging activity was

determined by measuring the absorbance at 517 nm against blank samples lacking compound. Methanol was used for the baseline correction. Lower absorbance of the reaction mixture indicates higher free radical scavenging activity [22]. The radical scavenging activity was expressed as the inhibition percentage and was calculated using the following formula:

$$\% \text{ Inhibition} = [(A_0 - A_1) / A_0] \times 100$$

Where A_0 is the absorbance of DPPH at 517 nm as a control and A_1 is the absorbance of DPPH in the presence of test sample. The result was compared to butylated hydroxy toluene (BHT) as standard.

2.4.2. Antibacterial Activity

The *in vitro* antibacterial activity of **2(a-h)** was evaluated against *Bacillus cereus* (PTCC 1556), *Staphylococcus aureus* (PTCC 1112), *Escherichia coli* (PTCC 1330) and *Klebsiella pneumonia* (PTCC 1053) by disc diffusion method [23]. Nutrient agar plates were inoculated with the overnight bacterial culture. The compounds were dissolved in DMSO and at concentration of 30µg/disc were placed on the surface of the inoculated plates. Amikacin (30µg/disc) was used as standard. The petri plates were incubated at 37°C for 24 h. Antibacterial activity was determined by measuring the diameter of inhibition zone.

3. Results and discussion

The synthesis route is shown in Fig.1. azo-azomethine dyes 2,2'-(1E,1'E)-(1,2,5-oxadiazole-3,4-diyl)bis(azan-1-yl-1-ylidene)bis(methan-1-yl-1-ylidene)bis(4-(phenyldi azenyl)phenol (**2a-h**) have been synthesized via condensation reaction of 2-hydroxy-5-(aryldiazenyl)benzaldehyde (**1a-h**) with 3,4-diamino-1,2,5-oxadiazole in methanol. All prepared dyes are air stable solids, soluble in DMSO, DMF and purified by recrystallization. The structures of all compounds were then characterized by elemental analysis, mass, IR, UV, ^{1}H and ^{13}C NMR spectroscopy. The presence of -CH=N-, –N=N- and OH functional

groups in structure of synthesized dyes makes which could potentially act as multidentate ligands and used in polymer

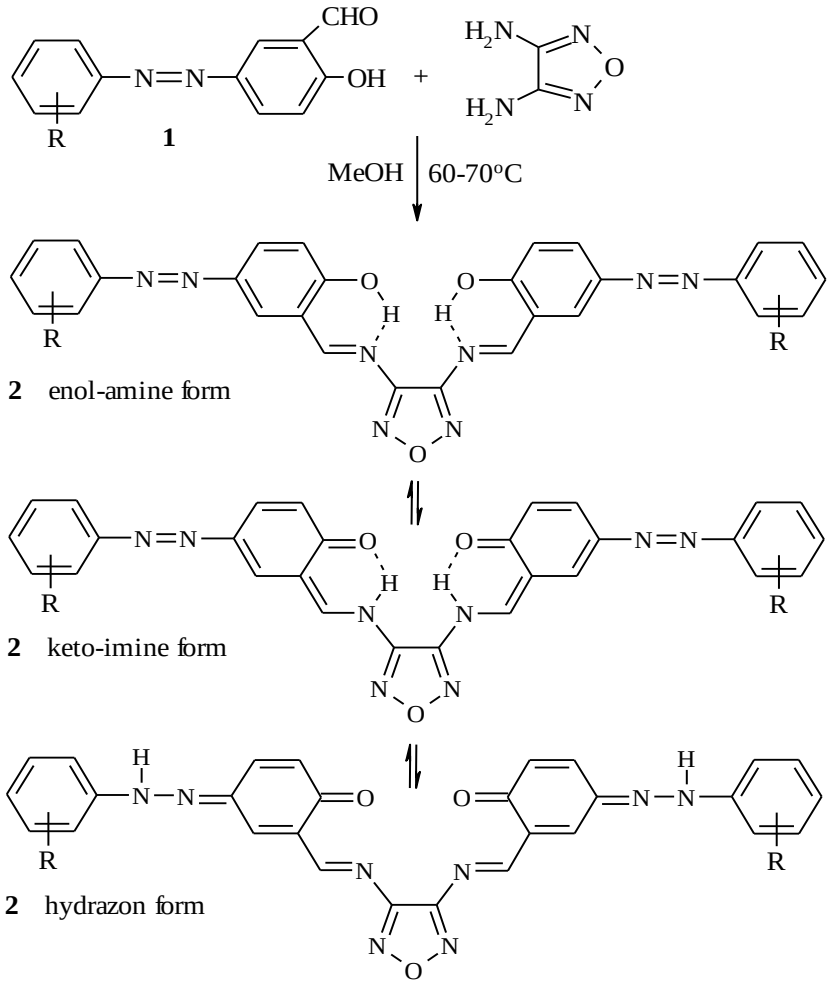

a) R=H **b**) R=4-Me **c**) R=4-Et **d**) R=3,5 di-Me
e) R=4-iPr **f**) R=4--OMe **g**) R=4-NO_2 **h**) R=4-SO_2-OH

Fig. 1: Synthesized **2** with azo precursors and the enol–keto tautomeric

3.1. Infrared spectra

The characteristic IR absorption bands of azo-azomethine Schiff base derivative **2a-h** were determined in KBr. The solid state FT-IR spectra of dye's **1a-h** showed C=O bands at range of 1660-1672 cm^{-1}[8, 19-20]. The absence of *ν*(C=O) absorption in the IR spectra of synthesized dyes together with the appearance of new *ν*(C=N) absorption in the range of 1610-1674 cm^{-1} indicated that new Schiff base compounds had been formed. The solid state

FT-IR spectra of dye's **2a-h** showed OH phenolic band at range of 3417-3460 cm^{-1}. The *v*(CH=N) and *v*(N=N) absorptions appeared in the range of 2840-2960 cm^{-1} and 1571-1583 cm^{-1}, respectively, which indicates the formation of Schiff bases of **2a-h**. The bands *v*(C-N), *v*(C-O) and *v*(N-O) vibrations are in the range of 1278-1296, 110-1163 and 1018-1045cm^{-1}, respectively. Also for **2f**, **2g** and **2h**, the azo-azomethine vibration is very sharp at 1635, 1652 and 1674 cm^{-1}, which corresponds to *v*(C=O) vibration. This might arise from existence of the hydrazone and/or enaminone tautomers of azo–azomethine compounds in the solid state. Another evidence for existence of the hydrazone and/or enaminone tautomers is phenolic *v*(C-O) vibration which observed at 1147-1155 cm^{-1} in compounds **2f-h,** and it is in agreement with results obtained for similar azo Schiff bases [12, 17-20]. The IR spectra of **2g** and **2h** show strong bonds at 1335 and 1521 cm^{-1} and/or 1184 and 1222 assigned for ν_s and ν_{as} of the NO_2 and SO_2 groups, respectively [2, 5, 8, 17-20, 24].

3.2. ^{1}H and ^{13}C NMR spectra

The NMR spectral results, obtained for Schiff base compounds **2a-h** at ambient temperature in DMSO-d_6, with the hydrogen assignments are presented in experimental section. The NMR analysis appeared to support the synthesis of all compounds. The ^{1}H NMR spectrum of **2a-h** exhibited D_2O exchangeable signals for the OH protons at δ_H 11.57-11.89 ppm. The CH=N proton signals appears in the range of 9.37-10.58 ppm. ^{1}H NMR spectra of azo–azomethine compounds **2b** and **2d-h** show two doublet at 7.99-8.12 ppm and 7.14-7.23 ppm, assigned to the *para*-substituted aromatic ring. The ^{13}C NMR spectra of **2a-h** consisted of twelve carbon peaks; One peak for CH=N, one peak for five member ring oxadiazole carbons and ten peak for benzene aromatic region. The CH=N, and five member ring oxadiazole carbons appear in the range of 162.58-163.80 and 156.38-157.48 ppm, respectively. Also for azo-azomethine dyes **2a-h**, the phenolic carbons (C-OH) appear at 167.00-171.83 ppm, which may be corresponds to C=O character. This might arise from

existence of the hydrazone and/or enaminone tautomers of azo–azomethine compounds and it is in agreement with results obtained for similar azo Schiff bases [8, 18-20, 24].

3.3. The electronic absorption spectra

The electronic spectra of compounds **2a-h** were measured (in the range of 300–600 nm) in four common solvents, MeOH, THF, DMSO and DMF at room temperature (Table 1). The UV–vis absorption spectra of compounds **2a-h**, in MeOH, THF, DMSO and DMF solvents display mainly two bands at 318-397 nm and 432-486 nm and give a red shift similar to the same spectra of azo- Schiff bases (Table 1). The broad band observed in the range of 432-486 nm can be assigned to an n→π* electronic transition of azo-aromatic chromophore and intramolecular charge transfer interaction such as the whole of dyes [8, 18-20, 25, 26]. The intramolecular charge transfer bands can be assigned to the existence of enol–keto equilibrium originating from hydrogen transferred form hydroxyl group to imine or azo nitrogen. The absorption curves of **2a-h** in DMF solvent are shown in Figure 2. The results indicated that the position π→π* band is influenced by the nature of the *para*-substitution (Table 1). The intensity of bands appeared at 318-397 nm bands are in the order, 2g >2h >2f >2e ≈2c >2d >2a >2b and 432-486 nm are in the order: 2g >2h >2f >2e >2c >2b >2a >2d respectively. When the NO_2, SO_3H and MeO groups was introduced in the aryl azo component, in lieu of hydrogen or alkyl groups, the absorption spectra give a considerable blue shift as other aryl azo-Schiff bases [18-20, 24-27]. This means that **2f-h** has a more extensive conjugation than others substitution (Table 1).

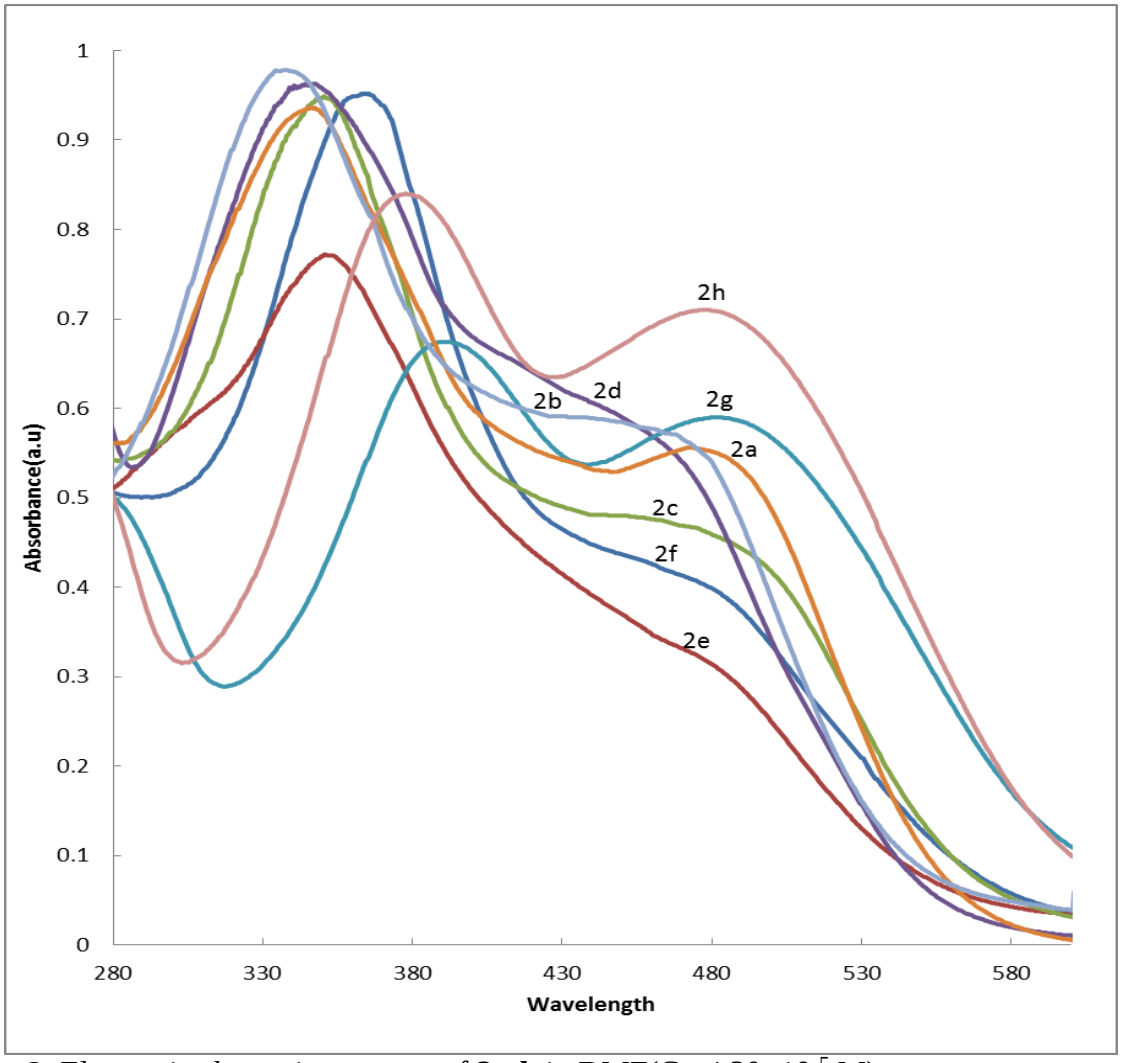

Fig. 2: Electronic absorption spectra of **2a-h** in DMF(C= 4.30×10^{-5} M) at room temperature.

Table 1: Summary of the UV-Vis absorption bands for compounds **2a-h**

compound	MeOH	THF	DMSO	DMF
2a	318(A=0.173), 442(A=0.036)	326(A=0.49), 451(A=0.19)	337(A=0.634), 460(A=0.059)	345(A=0.936), 473(A=0.556)
2b	319 (A=0.479), 439(A=0.399)	321(A=0.605), 445(A=0.437)	329(A=0.511), 453(A=0.323)	338(A=0.978), 468(A=0.571)
2c	330(A=0.699), 442(A=0.156)	339(A=0.566), 452(A=0.16)	346(A=0.836), 455(A=0.222)	350(A=0.949), 470(A=0.469)
2d	328(A=0. 412), 432(A=0.042)	331(A=0.423), 439(A=0.038)	338(A=0.476), 447(A=0.02)	343(A=0.962), 454(A=0.582)
2e	340(A=0.402), 449(A=0.158)	345(A=0.459), 459(A=0.174)	349(A=0.838), 476(A=0.25)	351(A=0.772), 475(A=0.324)
2f	341(A=0.437), 458(A=0.171)	345(A=0. 782), 465(A=0.154)	357(A=0.651), 474(A=0.247)	363(A=0.952), 478(A=0.402)
2g	-	383(A=0.481), 462(A=0.202)	397(A= 0.389), 477(A=0.252)	392(A=0.674), 486(A=0.589)
2h	360(A=0.476) 455(A=0. 022)	-	365(A=0.423) 468(A=0.057)	378 (A=0.840) 480 (A=0.701)

The solvatochromic behavior of a dye is the shift of the π→π* band wavelength due to the presence of solvent with different polarity which is due to the interaction between the solvent and solute [28]. The electronic spectra of 4.30×10^{-5} M solution of compounds **2a-h** were measured in three organic solvents with different polarity at room temperature (Table 1). The absorption bands at 345-363 nm and 462-481 nm, generally show bathochromic shift (positive solvatochromism) with polarity change of solvent (Fig. 3). We show that the solvatochromism may be due to the effect other causes such as dipole moment changes and the hydrogen bonding strength in polar solvents.

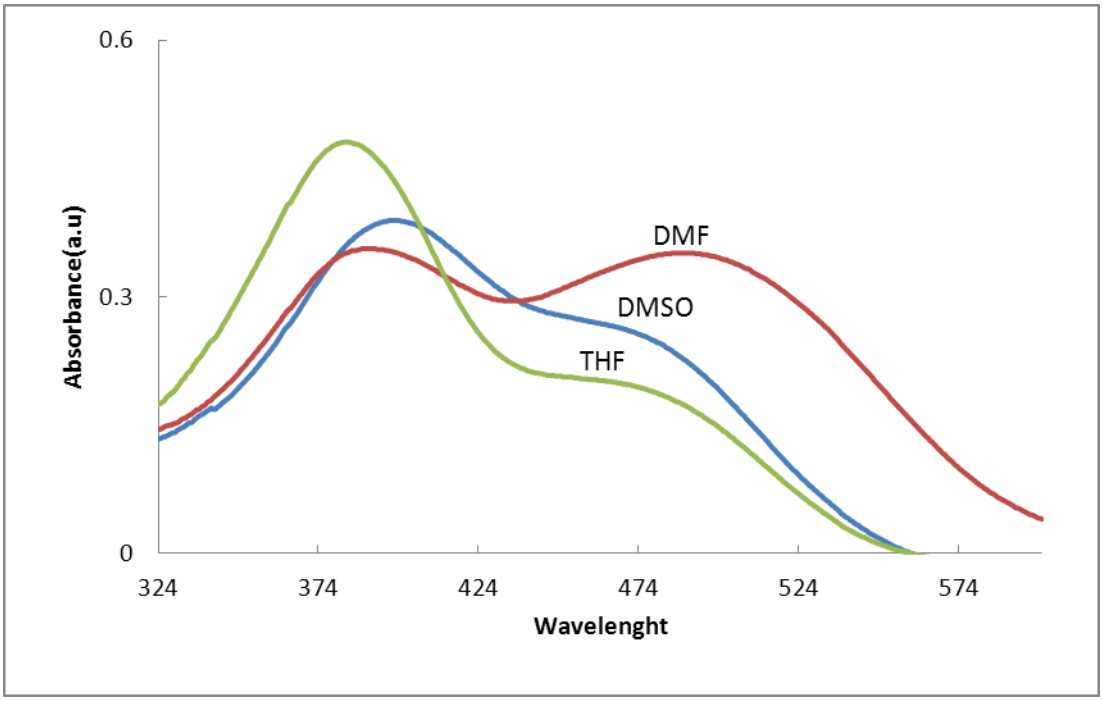

Fig. 3: Absorption spectra of **2g** in DMF, DMSO and THF solvents.

Furthermore, the absorption spectra of **2g** at different volume ratios of the applied pair of solvents DMF/H_2O were also recorded (Fig. 4). It was observed that the intensity of absorption of the band about 392 nm (probably enol-imine form) increased, while absorption of the band about 486 nm (keto-amine form) decreased with increasing of the volume content of water. This implies that there is enol–keto equilibrium, that it is dependent on polarity of solvent.

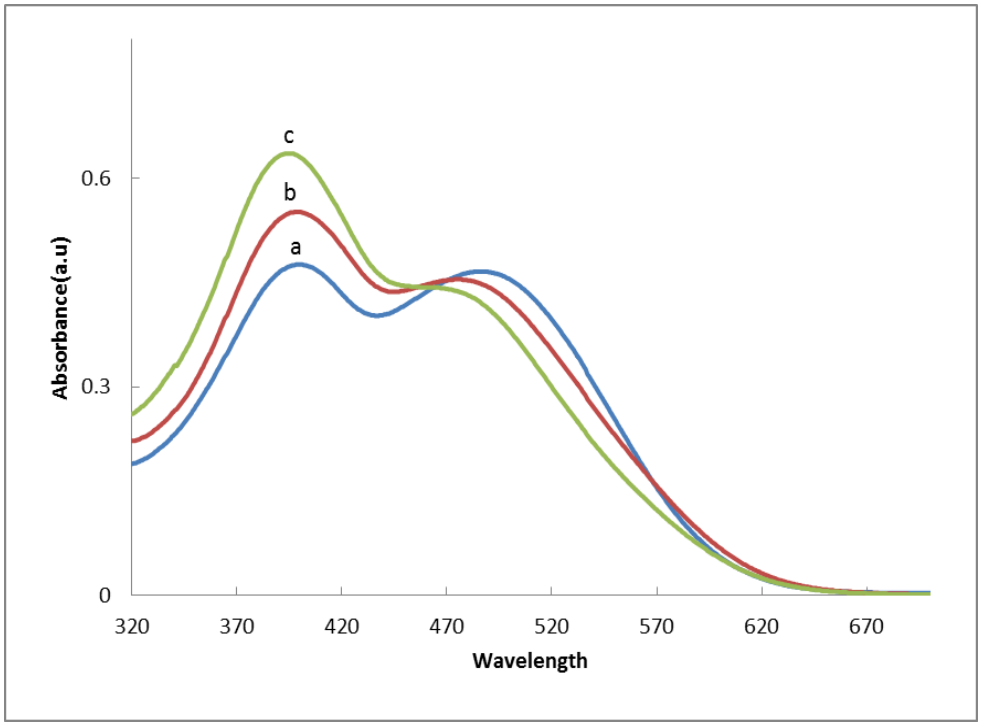

Fig. 4: Absorption spectra of **2g** in DMF (C= 4.3×10^{-5} M) and H_2O: (a) 0%; (b) 10% and (c) 30% water.

Also, the UV-visible spectrum of compound **2g** was measured in different pH (Fig. 4). It was observed that the intensity of absorption of the band about 392 nm (probably enol-imine form) decreased, while absorption of the band about 486 nm (keto-amine form) increased and show blue shift when the pH increased. It shows that enol-imine – keto-amine equilibrium is dependent on pH (Fig. 1).

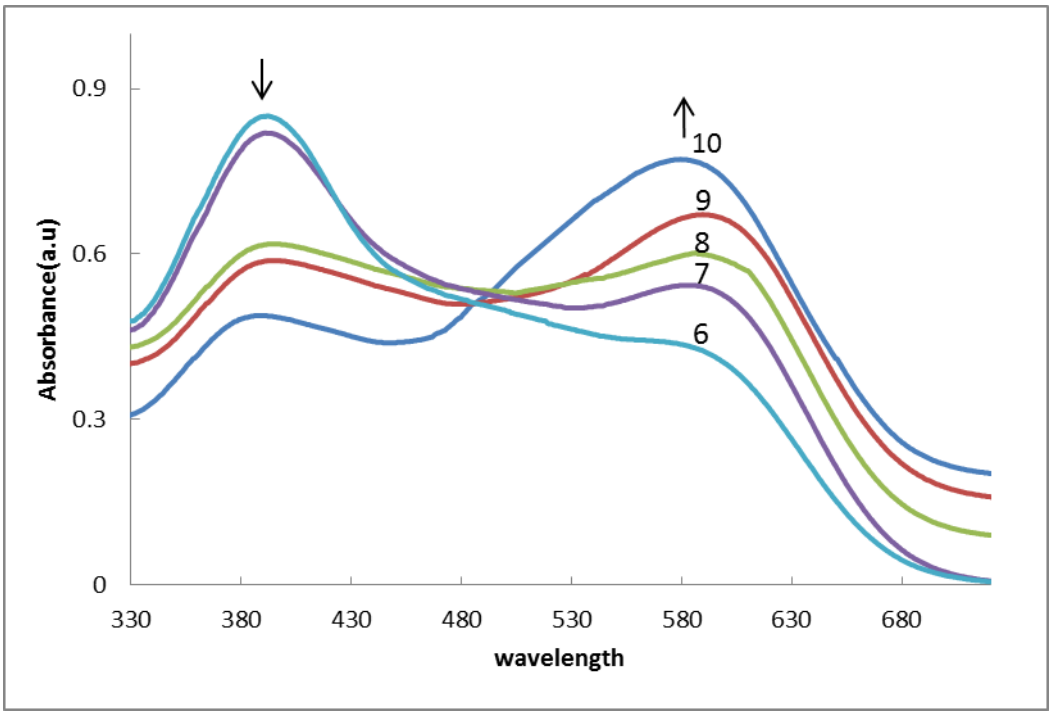

Fig. 5: Dependence of electronic absorption spectra of **2g** in DMF(C= 3.2×10^{-5} M) on different pH.

Therefore, the nature of substitutions, solvent environment, hydrogen bonds, temperature, pH and changes in the dipole moment of the molecules are the key factors in deciding the solvatochromism of azo-azomethine dyes [8, 19-20, 24].

3.4. Quantum Chemical Calculations

We could not obtain suitable crystals of synthesized compounds (**2a-c**) for X-ray diffraction work; therefore, we chose to assess its structural parameters by quantum chemical calculations using the gaussian 03 program [29-31]. The geometries of the compound **2a** were fully optimized using the B3LYP density functional theory (DFT) method with standard 6-311++G(2d,2p) basis set. Harmonic frequency calculations were performed at all the stationary points to characterize its nature and to ensure that the optimized structure corresponds to a global minimum. The vibrational band assignments were made using the Gauss-View molecular visualization program [32]. The representative structures and selected

optimized geometric parameters of compound **2a** and **2g** are given in Figures S1 and Table S2, (Supplementary data). The Quantum chemical calculations data indicated that dipole moment, bond lengths, bond and torsion angles of **2a** and **2g** are approximately similar (Table S2). The basic structural framework that contain three aromatic rings (phenyl, salicylaldehyde and oxadiazole), N=N and C=N linkage is found to be planar in the optimized structural of the compounds **2a** and **2g**. This allows the π-electron conjugation to extend throughout the aromatic rings.

The C_{12}-H_{15} distance of **2a** and **2g** are calculated to be 133.5 and 133.3 pm, respectively which is lower than the C-OH phenolic. Also, according to calculation the O_{15}-H_{15} and $H_{15}\cdots N_{17}$ distances of these molecules are 98.8, 98.9 pm and 175.6, 175.2 pm, respectively. optimized structures of **2a** and **2g** indicate the formation of a strong O_{15}-H_{15} $\cdots N_{17}$ hydrogen bond which are much shorter than the sum of the van der Waals radii of nitrogen (155 pm) and hydrogen (120 pm). It indicates the presence of hydrogen bonding interactions between the O–H bond and the nitrogen atom of the CH=N group. However, the red shift of O-H stretching frequency provides further indication of this hydrogen bonding. Results show that the hydrogen bonding in **2g** is partially stronger than **2a.** its indicate that hydrogen bonding depends on substitution effcts.

The O–H stretching frequency in compound **2a** and **2g** appears at aboat 3430 cm^{-1}, which are lower than the experimental value (3657 cm^{-1}) of the O–H stretching frequency in phenol [20]. The C=N stretching vibrational frequency for **2a** and **2g** (1610, 1633 cm^{-1}, respectively) is found to be almost unchanged in compound 2a.

The calculated C=N stretching frequency (1661 cm^{-1}) is in agreement with the experimental value of 1633 cm^{-1}. It is difficult to determine precisely the O–H stretching frequency for the hydrogen bonded O–H, because of the well-known broadening effect.

Table S2: Selected bond lengths, bond angles and torsion angles for optimized structures B3LYP/6-311++G(2d, 2p) of **2a** and **2g**		
Compounds	**2a**	**2g**
μ	1.6677	٢,٨٩٧٥
Bond lengths(Å)		
C_1-N_7	1.417	1.417
N_7-N_8	1.252	1.252
N_8- C_9	1.413	1.410
C_9-C_{10}	1.404	1.405
C_{12}-C_{13}	1.425	1.426
C_{12}-O_{15}	1.335	1.333
O_{15}-H_{15}	0.988	0.989
C_{13}-C_{16}	1.441	1.442
C_{16}-N_{17}	1.292	1.292
N_{17}…H_{15}	1.756	1.752
N_{17}-C_{18}	1.382	1.382
C_{18}-N_{19}	1.306	1.306
N_{19}-O_{20}	1.372	1.372
Bond angles (°)		
C_1-N_7-N_8	115.49	115.17
C_9-N_8-N_7	115.43	115.61
C_{10}-C_9-C_{14}	118.93	119.02
C_9-C_{14}-C_{13}	120.95	120.90
C_{11}-C_{12}-C_{13}	119.40	119.47
C_{12}-C_{13}-C_{14}	119.27	119.25
C_{14}-C_{13}-C_{16}	119.09	119.13
C_{13}-C_{12}-O_{15}	121.96	121.90
C_{11}-C_{12}-O_{15}	118.63	118.62
C_{13}-C_{16}-N_{17}	122.26	122.16
C_{16}-N_{17}-C_{18}	119.74	119.76
Torsion angles(°)		
C_2-C_1-N_7-N_8	179.85	179.85
C_1-N_7-N_8-C_9	179.96	179.95
N_7-N_8-C_9 –C_{10}	-179.90	-179.76
C_{13}-C_{16}-N_{17}- H_{15}	-0.5411	-0.4118
C_{11}-C_{12}-O_{15}-H_{15}	179.36	179.50
C_{13}-C_{12}-O_{15}-H_{15}	-0.5550	-0.4244
C_{16}-C_{13}-C_{12}-O_{15}	-0.1983	-0.2559
C_{14}-C_{13}-C_{16}-N_{17}	-179.21	-179.36
C_{13}-C_{16}-N_{17}- C_{18}	-176.73	-176.77
$\mathbf{C_{16}}$-$\mathbf{N_{17}}$-$\mathbf{C_{18}}$-$\mathbf{N_{19}}$	28.868	27.882
N_{19}-C_{18}-N_{17}-H_{15}	-145.23	-146.50

3. 4. Biological activities

The antioxidant activity of newly synthesized compounds was evaluated using DPPH radical scavenging method. The results indicated that the compounds **2a-g** exhibited moderate to mild antioxidant effect (Table 2). Compound **2e** bearing an isopropyl group on the phenyl ring showed maximum antioxidant activity and least activity was observed for **2g** bearing a nitro group in the same position. Obtained results revealed that compounds substituted with electron donating groups increased the scavenging /antioxidant activity. The results for antibacterial activity revealed that synthesized compounds showed varying degree of inhibition against *B. cereus* and *S. aureus* strains (Table 3). However, *E.coli* and *K. pneumonia* were not sensitive to any of the test samples. In compounds substituted with Alkyl groups antibacterial activity was increased, while the activity decreased when nitro or methoxy groups were substituted. Compound **2d** (bearing two methyl groups in the 3 and 5 positions on the aromatic ring) showed higher activity than other test compounds. This activity may be correlated with the greater lipophilic nature of the compound which subsequently favors its permeation through the lipoid layer of the bacterial membrane.

Table 2: Antioxidant activity of **2a-g** (1mg/ml)

Compound	% Inhibition
2a	5.0
2b	7.0
2c	16
2d	17
2e	28
2f	11
2g	1.0
BHT	92.1

Table 3: Antibacterial activity of **2a-g**		
Compound 30 (μg/disc)	Zone of inhibition(mm)	
	B.cereus	*S.aureus*
4a	10	11
4b	13	12
4c	12	13
4d	8	10
4e	12	13
4f	12	11
4g	9	9
Amikacin	25	21
DMSO	-	-

4. Conclusion

A series of azo-azomethine dyes based on oxadiazole rings were synthesized by condensation reaction of 5-((4-R-phenyl)diazenyl)-2-hydroxybenzaldehyde with 3,4-diamino-1,2,5-oxadiazole. Substitution, solvent environment and acid-base influence on the wavelength of electronic absorption have been studied. The absorption maxima of synthesized dyes show bathochromic shift (positive solvatochromism) in DMF and DMSO than THF solvent. Obtained results revealed that compounds substituted with electron donating groups increased the scavenging /antioxidant activity.

References

[1] Borisova NE, Reshetova MD, Ustynyuks YA. Metal-Free Methods in the Synthesis of Macrocyclic Schiff Bases. Chem. Rev. 2007;107:46-79.

[2] Kim YD, Cho JH, Park CR, Choi JH, Yoon C, Kim JP. Synthesis, application and investigation of structure–thermal stability relationships of thermally stable water-soluble azo naphthalene dyes for LCD red color filters. Dyes and Pigments 2011;89:1-8.

[3] Qian Y, Wang G, Xiao G, Lin B, Cui Y. The first order molecular hyperpolarizability and thermal stability of charge –transfer azo diol and azo aldimine. Dyes and Pigment 2007;75:460-465.

[4] Pinna R, Jamme F, Rutten FJM, Smith EF, Willis MR, Briggs D, McCoustra MRS. Towards a fully optimized organic LED device: Analysis of surface synthesis using coupling reactions by ToF-SIMS. Appl. Surf. Sci. 2006;252:6672-6675.

[5] Asgari-sabet R, Khoshsima H. Real-time holographic investigation of azo dye diffusion in a nematic liquid crystal host. Dyes and Pigments 2010;87:95-99.

[6] Behpour M, Ghoreishi SM, Soltani N, Salavati-Niasari M, Hamadanian M, Gandomi A. Electrochemical and theoretical investigation on the corrosion inhibition of mild steel by thiosalicylaldehyde derivatives in hydrochloric acid solution. Corrosion Science 2008;50:2172-2181.
[7] Durmus F, Atahan A, Zengin M. Synthesis, Characterization and electrochemical behavior of ONS type tridentate Schiff base. Spectrochimica Acta Part A. 2011;84:1-5.
[8] Odabasoglu M, Albayrak C, Ozkanca R, Aykan FZ, Lonecke P. Some polyhydroxy azo–azomethine derivatives of salicylaldehyde: Synthesis, characterization, spectroscopic, molecular structure and antimicrobial activity studies. J. Mol. Structure 2007; 840:71-89.
[9] Iwan W, Sek D. Processible polyazomethines and polyketanils: From aerospace to light-emitting diodes and other advanced applications. Prog. Polym. Sci. 2008;33:289-345.
[10] Anand P, Patil VM, Sharma1 VK, Khosa RL, Masand N. Schiff bases: A Review on Biological Insights. International Journal of Drug Design and Discovery 2012;3:851-868.
[11] Kumar H, Chaudhary RP. Biological studies of a novel azo based Heterocyclic Schiff base and its transition metal complexes. Der Chemica Sinica. 2010;1:55-61.
[12] Kakanejadifard A, Esna-ashari F, Hashemi P, Zabardasti A. Synthesis and characterization of an azo dibenzoic acid Schiff base and its Ni(II), Pb(II), Zn(II) and Cd(II) complexes. Spectrochimica Acta Part A. 2013;106:80–85
[13] Sheremetev A, Makhova A. Monocyclic Furazans and Furoxans. Advances in Heterocyclic Chemistry, 2001;78:65-188.
[14] Rajak H, Kharya MD, Mishra P. Biological activity of oxadiazoles, International Journal of pharmaceutical science and nanotechnology. 2009;2:390-406.
[15] Oliveira CS, Lira BF, Barbosa-Filho MB, Lorenzo JGF, Athayde-Filho PF. Synthetic approaches and pharmacological activity of oxadiazoles. Molecules 2012;17:10192-10231.
[16] Muhi-eldeen Z, Juma'a G, Al-kaissi E, Nouri L. Antimicrobial activity of some new oxadiazole derivatives. Jordan Journal of Chemistry 2008;3:233-243.
[17] Ogawa K, Harada J. Aggregation controlled proton tautomerization in salicylideneanilines. J. Mol. Structure 2003;647: 211-216.
[18] Khanmohammadi H, Erfantalab M, Azimi G. New acyclic 1,2,4-triazole-based Schiff base hydrazone: Synthesis, characterization, spectrophotometric and computational studies. Spectrochimica Acta Part A. 2013;105:338-343.
[19] Kakanejadifard A, Azarbani F, Zabardasti A, Rezayat A, Ghasemian M, Kakanejadifard S. Spectroscopic and solvatochromism studies along with antioxidant and antibacterial activities investigation of 2-((2-mercaptophenylimino)methyl)-4-(phenyldiazenyl)phenol. Spectroscopic Chem. Acta Part A. 2013;114:404–409.
[20] Kakanejadifard A, Azarbani F, Zabardasti A, Kakanejadifard S, Ghasemian M, Esna-ashari F, Omidie S, Shirali S, Rafieefar M. Dyes and Pigments 2013;97:215-221.
[21] Shimada K, Fujikawa K, Yahara K, Nakamura T. Antioxidative properties of xanthin and autooxidation of soybean oil in cyclodextrin emulsion. J. Agri. and Food Chem. 1992;40:945–948.
[22] Viraj PJ, Kiran MP, Ravikumar V, Modi, DR, Badmanaban and Dhrubo JS. In-vitro antioxidant assay of synthesized 2 & 4 substituted phenyl urea/theorem (carboxylic acid/carboxamide) by using 1,1-diphenyl-2-picrylhydrazyl as a stable oxidant. International Journal of Drug Development and Research 2011;3(4):294-299.
[23] Bauer AW, Kirby WMM, Sherris JC, Turck M. Antibiotic susceptibility testing by a standardized single disk method. Am. J. Clin. Pathol. 1966;45:493-496.

[24] Khanmohammadi H, Rezaeian K. Thermally stable water insoluble azo-azomethine dyes: synthesis, characterization and solvatochromic properties. Spectrochimica Acta Part A. 2012;97:652-658.
[25] Karc F, Sener N, Yamac M, Sener I, Demiralih A. The Synthesis, antimicrobial activity and absorption characteristics of some novel heterocyclic disazo dyes. Dyes and Pigments 2007;80: 47-52.
[26] Sheikhshoaie I, Saheb V, A new salen base 5-(phenylazo)-N-(2-amino pyridine) salicyliden Schiff base ligand: Synthesis, experimental and density functional studies on its crystal structure, FT-IR, ^{1}H NMR and ^{13}C NMR spectra. Spectrochimica Acta Part A. 2010;77:1069-1076.
[27] Khanmohammadi H, Darvishpour M. New azo ligands containing azomethine groups in the pyridazine-based chain: Synthesis and characterization. Dyes and Pigments 2009;81:167-173.
[28] Reicharedt C, Welton T. Solvents and Solvent Effects in Organic Chemistry, Fourth ed, VCH, 2011.
[29] Schlegel HB. Effect of electron correlation on theoretical vibrational frequencies. J. Comput. Chem 1982;3:234–250.
[30] Peng C, Ayala PY, Schlegel HB, Frisch MJ. Using redundant internal coordinates to optimize equilibrium geometries and transition states. J. Comput. Chem 1996;17:49-56.
[31] Frisch MJ, Trucks GW, Schlegel HB, Scuseria GE, Robb MA, Cheeseman JR, Montgomery Jr. JA, Vreven T, Kudin KN, Burant JC, Millam JM, Iyengar SS, Tomasi J, Barone V, Mennucci B, Cossi M, Scalmani G, Rega N, Petersson GA, Nakatsuji H, Hada M, Ehara M, Toyota K, Fukuda R, Hasegawa J, Ishida M, Nakajima T, Honda Y, Kitao O, Nakai H, Klene M, Li X, Knox JE, Hratchian HP, Cross JB, Bakken V, Adamo, Jaramillo J, Gomperts R, Stratmann RE, Yazyev O, Austin AJ, Cammi R, Pomelli C, Ochterski JW, Ayala PY, Morokuma K, Voth GA, Salvador P, Dannenberg JJ, Zakrzewski VG, Dapprich S, Daniels AD, Strain MC, Farkas O, Malick DK, Rabuck AD, Raghavachari K, Foresman JB, Ortiz JV, Cui Q, Baboul AG, Clifford S, ioslowski J, Stefanov BB, Liu G, Liashenko A, Piskorz P, Komaromi I, Martin RL, Fox DJ, Keith T, Al-Laham MA, Peng CY, Nanayakkara A, Challacombe M, Gill PMW, Johnson B, Chen W, Wong MW, Gonzalez C, Pople JA, Gaussian 03, Revision E.01, Gaussian, Inc., Wallingford, CT; 2004.

[32] Dennington R, Keith T, Millam J. GaussView, Version 4.1.2, Semichem, Inc., Shawnee Mission KS; 2007.